

Design and Analysis of MEMS-Based Capacitive Power Inverter Using Electrostatic Transduction

Salih Rahmi Turan, Osman Ulkir and Melih Kuncan


Abstract—In this study, a capacitive microelectromechanical system (MEMS) based DC/AC power inverter design for renewable energy applications is proposed, and analyzed. In the proposed approach, electrostatic actuation is preferred to develop a DC/AC power inverter with varying phase overlap lengths for solar energy systems. The developed inverter is based on MEMS to achieve miniaturized performance, producing smooth sine wave output, efficiently obtaining the signal frequency, and low power consumption. The proposed inverter has a thickness of 325 μm , an active settlement area of 45x45x0.585 mm^3 , and an initial capacitance value of 2.9 pF. In addition, a 50-Hz mechanical resonance frequency was used to be compatible with the frequency of the city network. It can convert voltage values between 0.5 V and 24 V DC with a MEMS power inverter. Because the inverter is based on a capacitive structure, it provides near-zero power consumption. The frequency and waveform of the converted DC/AC signal match the AC signal of a power grid with an efficiency of 5%.

Index Terms—Electrostatic actuation, MEMS, miniaturization, power inverter, renewable energy.


I. INTRODUCTION

THE DEMAND in the renewable energy market is increasing every year. Solar energy systems are one of the most promising renewable energy generation technologies. The primary purpose of these systems is to reduce costs and increase efficiency [1]. Power inverters are one of the essential considerations in most alternative energy systems for converting DC energy from photovoltaic generators to AC energy. Today, various studies are being conducted to increase the efficiency of these high-order power inverters [2-4]


Salih Rahmi Turan, is with Institute of Science, Siirt University, Siirt, Turkey (e-mail: srahmituran@hotmail.com).

 <https://orcid.org/0000-0001-5826-0786>

Osman Ulkir, is with Department of Electric and Energy, Mus Alparslan University, Mus, Turkey (e-mail: o.ulkir@alparslan.edu.tr).

 <https://orcid.org/0000-0002-1095-0160>

Melih Kuncan, is with Department of Electric and Electronics Engineering, Siirt University, Siirt, Turkey (e-mail: melihkuncan@siirt.edu.tr).

 <https://orcid.org/0000-0002-9749-0418>

Manuscript received Jan 14, 2024; accepted Mar 17, 2024.

DOI: [10.17694/bajece.1419596](https://doi.org/10.17694/bajece.1419596)

Commercial transducer systems consist of power electronic switches made of semiconductors such as silicon carbide (SiC) or gallium nitride (GaN) [5, 6]. However, these systems have disadvantages such as on-state loss, switching loss of power devices, complex control system configurations, low efficiency, and high costs. All of these disadvantages are partially eliminated by PWM inverters [7]. Particularly popular in medium and high power applications, the multilevel inverter has many switches to control. This number of switches increases the probability of failure of the power electronics driving circuit. A multilevel inverter generates a sine wave associated with harmonics that depend on the switching frequency in power electronics [8-10]. These harmonics cause high leakage current and high-frequency noise, affecting the PV power system performance and causing easy failure of the PV power system [11, 12]. Today, the improvement of inverter systems is to develop DC/AC inverter performance, increase the temperature to improve reliability, increase the operating voltage to adapt to high-voltage PV systems, improve frequency regulation, and reduce cost [13-15].

Recent studies have offered approaches to overcome the harmonic problem and other shortcomings of the power inverters [16-18]. These approaches faced issues such as cumbersome and expensive, a large number of auxiliary switches increasing system complexity, high voltage stress of switches, large size and weight of passive components, and complex control system. In addition, the electromechanical power inverter method has been proposed as an alternative to the power electronics inverter [19, 20].

Microelectromechanical systems (MEMS) will contribute to the development of power inverters because they offer an approach to the miniature bulk device, high efficiency, and low-cost manufacturing [21, 22]. This approach is a micro processing technology used since the late 1980s. MEMS technology has many applications, such as radio frequency, accelerometer gyroscope, sensor and actuator technology, biomedical, thermodynamics, telecommunications, and so on [23-26]. Electrostatic actuation is the most important for MEMS technology, which has different actuation methods such as piezoelectric, electromagnetic, and thermal principles [27, 28]. MEMS DC/AC capacitive power inverters are comb-driven electrostatic actuators commonly used in MEMS applications, consisting of two interconnected finger structures. One comb is fixed, and the other is attached to a compatible

suspension [29, 30]. The inclusion of this structure in solar PV system will significantly improve power inverter technologies because of its miniature size, high efficiency and faster response, lower production cost, and lower power consumption [31, 32].

This paper presents a new capacitive electromechanical power inverter's modeling, design, and simulation results. This study aims to obtain information about the compatibility of MEMS inverter with the system by voltage time analysis and to convert DC voltage to AC voltage in the form of a smooth sinusoidal wave by using the solar energy system. The suggested MEMS design is based on a comb drive structure for generating two sets of the variant capacitor. One with two sets of electrodes where one is moving and the other is fixed. Because the designed MEMS system is capacitive based, there will be no need for power consumption in the conversion process. The MEMS capacitive resonator structure provides the sensitivity and mass detection of electrons, and low frequency, low power consumption, low cost, and minimum power loss are targeted. Based on the results obtained, it is predicted that it can be used in different electronic applications. Modeling and simulation studies of MEMS power inverter were made using modelling software.

II. MATERIALS AND METHODS

A. Structural Design of MEMS Power Inverter

The MEMS-based DC/AC power inverter is structurally designed with a mechanical resonator and variable capacitors. The mechanical resonator consists of a seismic mass. Electrodes surround these masses to form the moving part of the variable capacitors (Fig. 1). MEMS resonators have been used in sensor design for many years. These resonators actively perceive mass, force, and electronic transformations and adapt to the system. The variable capacitor forms the intertwined moving part with adjacent electrodes in the seismic mass. As it can be understood from here, the seismic mass will be sensitive to mechanical vibration and cause a mechanical displacement.

The design consists of fixed comb electrodes, moving comb electrodes, a proof mass suspended by double folded flexure beams, and a shuttle mass. The electrons fixed to the anchors are composed of the electrons in the moving combs and the mass suspended by the beams (Fig. 1). Here, deviations occur because it creates a capacitive effect on the moving parts. This means that as the capacitance on one side increases, the capacitance on the other will also increase. One of the two capacitors formed here acts as a driver capacitor, while the other acts as a converter. When the comb structure is examined, it should be designed so that one of the fingers on the moving part is extended while the other is short. Because it reduces deviations, it is exposed to and enables us to obtain more capacitance formation.

MEMS capacitors were mechanically examined in two groups. These are differential variable capacitors or follower variable capacitors. The design in Fig. 1 is a follower variable capacitor type MEMS device [33].

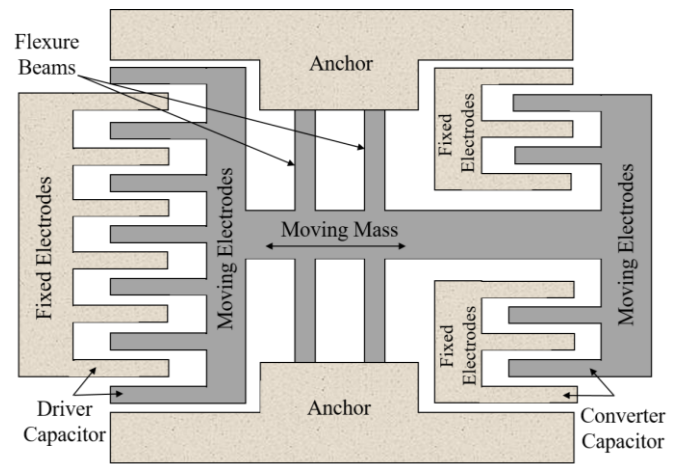


Fig.1. The design of the proposed MEMS power inverter

Differential variable capacitors have two independent stators. However, as the rotor is rotated, the capacity of one section of the differential variable capacitor increases while that of other section decreases [34]. This keeps the capacitance constant while maintaining the sum of the two stators. These capacitors can therefore be used in capacitive potentiometric circuits. In follower variable capacitors, both capacitance devices exhibit simultaneous in- phase capacitance variation.

Mechanical movement of the seismic mass in the MEMS device can be achieved in two ways. One is accomplished by creating vibration with an external force, as in accelerometers and energy storage circuits [35]. The other is applying an external AC signal as MEMS resonators [36]. In this study, the capacitive MEMS device to be operated electrostatically is powered by an electrical AC signal to implement DC/AC power conversion. Because the AC voltage used in the city network in our country is 50 Hz and 220V, the frequency is taken as 50 Hz in this study. In addition, the classical MEMS settlement area was preferred. The design specifications are demonstrated in Table I.

TABLE I
DESIGN SPECIFICATIONS OF THE MEMS INVERTER

Sl. No.	Specification	Values
1	Active settlement area	$45 \times 45 \times 0.585 \text{ mm}^3$
2	Maximum mechanical deflection	15 μm
3	Driver initial capacitance	92 fF
4	Reference AC voltage	120 V
5	Load resistance	100 M Ω
6	Solar DC input	24 V
7	Frequency	50 Hz

B. Operating Principle of MEMS Power Inverter

Using the proposed MEMS technology, a capacitance-based power inverter was modeled, and simulation studies were carried out. The implementation of DC/AC conversion to the designed inverter system is given in Fig. 2a. MEMS transducers operate based on the principle of converting mechanical signals into electrical signals or vice versa on a miniature scale.

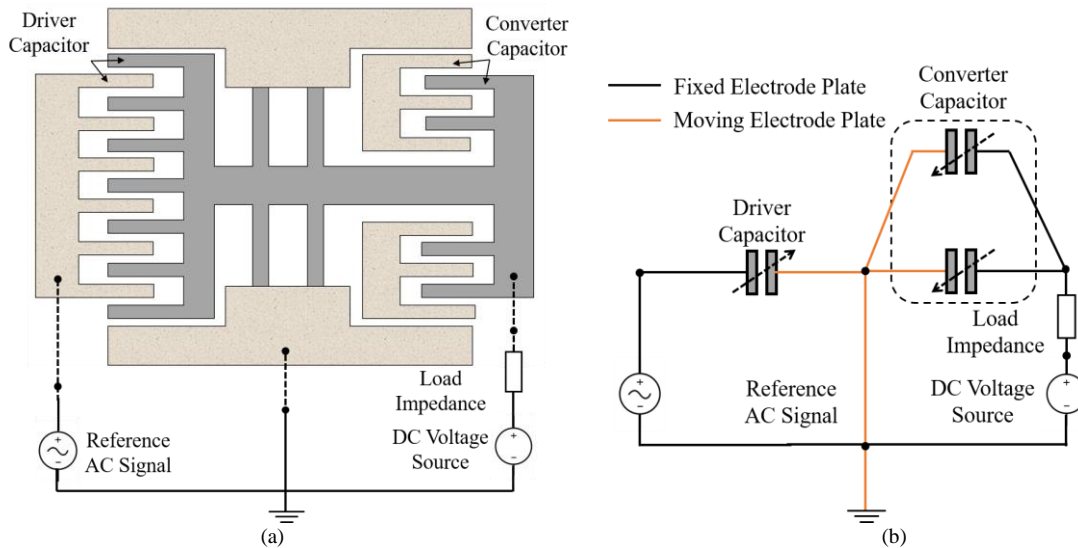


Fig.2. Capacitive MEMS power inverter (a) System implementation (b) Equivalent electrical circuit diagram

These transducers typically consist of tiny structures etched from semiconductor materials like silicon, incorporating mechanical components such as beams, diaphragms, or cantilevers, along with electrical components like capacitors or piezoelectric materials. When subjected to mechanical stimuli like pressure, acceleration, or vibration, these structures undergo minute physical deformations, resulting in changes in electrical properties, such as capacitance, resistance, or voltage.

The power inverter converts the DC signal from the solar system to AC usable signal. It is sufficient to apply a small AC signal to the MEMS switch input for the system to work. The DC voltage generated by the solar cell is applied to the MEMS device, and a converter capacitance is generated through the driver capacitance. These data are isolated in the ground section. Changing the reference AC signal here causes the efficiency of the converted DC/AC signal and the system to change.

The equivalent electrical circuit diagram of the system is shown in Fig. 2b. Here, the reference AC signal is connected in parallel with the driver capacitor. This AC signal induces an alternating electrostatic force across the driving capacitor electrodes, causing mechanical displacement of the seismic mass. In this case, the converter leads to the same deflection of the capacitor electrodes. As a result, a change in capacitance occurs. Electrically, the capacitance change of the DC converter capacitor induces an AC electric current. This current is expressed as the converted DC/AC current flowing through the load. Thanks to the ground that provides the electrical isolation between the driver and the converter capacitors, it prevents the reverse flow of AC current, which allows us to accept the power consumption as zero theoretically.

The photovoltaic systems are off-grid and on-grid photovoltaic systems connected to the grid. In the grid-connected system, the electricity produced by the solar panels is arranged in the grid-connected inverter, and the conversion is performed to be transferred to the electricity grid. If the battery is not used in these systems, the photovoltaic system may be

disabled in case of a power outage in the network. The battery support is required in grid-connected photovoltaic systems.

In systems separate from the grid, the electricity produced by the solar panels is regulated by the charge controller and stored in the batteries. The electricity stored in the batteries as DC is converted into AC electricity with the help of inverters. As can be understood from both systems, the direct current produced by the solar panels should be converted into alternating current with the help of DC/AC inverters. This study aims to obtain an efficient power inverter by integrating MEMS technology into a classical photovoltaic system. A block diagram representing a MEMS power inverter system has been incorporated into the conventional solar PV system (Fig. 3).

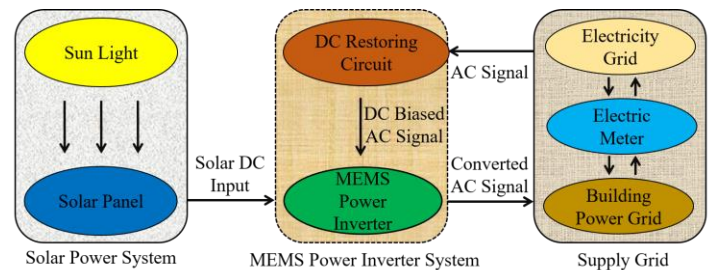


Fig.3. Solar PV system with MEMS power inverter unit

C. Mathematical Modelling of MEMS Power Inverter

The implementation of DC/AC conversion to the designed MEMS inverter system is shown in Fig. 2a. The basic modeling of the MEMS power inverter design is based on the electrical and mechanical electrostatic field approach in mechanical resonators. This approach consists mass-spring-damper system, variable capacitor, and electrical circuit. The model consists of seismic mass, mechanical springs, damping element, and mechanical stop (Fig. 4). The model variable capacitors are driver capacitor C_1 , and converter capacitor C_2 . The electrical circuit in the model consists of the load impedance Z_L , reference AC voltage source V_{AC} , and a solar DC input voltage source V_{DC} . The model can be mathematically symbolized by extracting the system force balance equation as follows [37]:

$$m_m \ddot{x}_m + b_m \dot{x}_m + k_m x_m = \vec{F}_{ex} + \vec{F}_s + \vec{F}_{es} \quad (1)$$

Here m_m is the total mass amount, b_m is the viscosity damping coefficient, k_m is the mechanical spring constant, and k_s is the mechanical stop constant. The symbol F_{ex} is external mechanical stimulation caused by mechanical vibration. In this study, the external mechanical excitation force is considered to be zero. Because external vibration is neglected. The symbol F_s is the mechanical stopping force vector formed by the seismic mass. This force value is calculated as follows:

$$F_s = k_s x_s \quad (2)$$

$$F_s = \begin{cases} 0, & -x_s \leq x \leq x_s \\ k_s(x + x_s), & x < -x_s \\ k_s(x - x_s), & x > x_s \end{cases} \quad (3)$$

Here x_s denotes the displacement of the mechanical stop. The expression F_{es} in equation 1 is the total electrostatic force. This force is proportional to the square of the applied voltage. A capacitance variation is observed here because the electrostatic force will cause displacement in the overlapping length. Capacitance is inversely proportional to voltage [38]. Therefore, the proposed MEMS inverter system is a compatible design in low-power applications and is suitable for low-cost, and low-power applications. This force is usually calculated based on the capacitance variation (C) and the capacitor voltage (V). The derivative of this variation gives the resonator deviation ($\frac{dC}{dx}$).

$$F_{es} = \frac{1}{2} \cdot \frac{dC}{dx} \cdot V^2 \quad (4)$$

The calculation of the capacitance in equation 3 depends on the geometry of the capacitor. For the variable capacitor shown in Fig. 2, the overlap area between the electrodes is the variable parameter. In line with these parameters, the capacitance is calculated as follows:

$$C = \frac{2\varepsilon_0 \varepsilon_r N_e (L_0 + \bar{x}) + t_e}{g} = C_0 \left(1 + \frac{\bar{x}}{L_0}\right) \quad (5)$$

In this equation, ε_0 is the permeability of the vacuum, ε_r is the middle dielectric constant, N_e is the number of electrons in the moving capacitor, L_0 is the first overlapping length of the electrode, t_e is the thickness of the electrode, g is the gap between the moving and fixed electrodes.

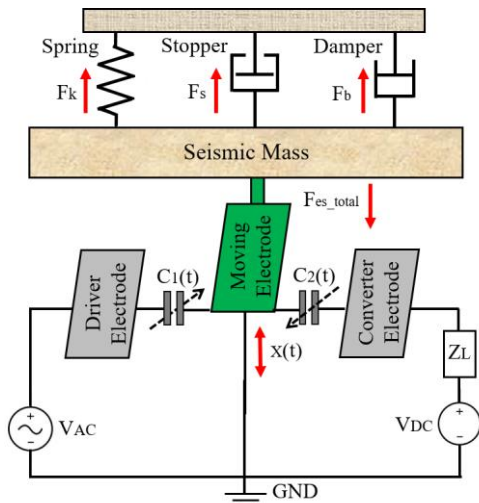


Fig.4. Electromechanical model of proposed MEMS power inverter

Capacitors work with DC voltage using charging and discharging methods. When it is full, it will work like an open circuit, so the current will be zero. When AC voltage is applied, it behaves like a resistor and changes depending on the frequency and capacitance of the capacitor. The symbol \bar{x} in equation 5 represents the deviation vector. This value can have a positive or negative sign depending on the displacement direction of the electrons. Accordingly, the resonator deflection of the capacitor changes as follows:

$$\frac{dC}{dx} = \begin{cases} \frac{C_0}{L_0}; \bar{x} = x \\ \frac{C_0}{L_0}; \bar{x} = -x \end{cases} \quad (6)$$

For the proposed MEMS power inverter, using the formula in equation 4, the total electrostatic force is calculated as follows. This force depends on the derivatives of the driver and converter capacitors and the square of their voltage.

$$F_{es_total} = \frac{1}{2} \left(\frac{dC_1}{dx} V_{C_1}^2 \mp \frac{dC_2}{dx} V_{C_2}^2 \right) \quad (7)$$

The voltages of the variable capacitors in the MEMS inverter are affected by the response of the electrical circuit. As can be seen from the simplified electromechanical model in Fig. 4, due to the parallel connection of the driver capacitor and the AC reference voltage, the voltage on the driver capacitor V_{C_1} is equal to the reference AC voltage V_{AC} . Calculating the voltage across the converter capacitor V_{C_2} is obtained by applying Kirchhoff's voltage law in the loop of the elements connected in series. According to this law, the algebraic sum of the potential differences in any loop must equal zero. Here, the DC voltage source is V_{DC} , load impedance Z_{LC} and converter capacitor C_2 are connected in series (Fig. 4). As a result, equation 8 is calculated as follows:

$$V_{C_2} = V_{DC} - i(t)Z_L \quad (8)$$

The converter voltage in equation 8 is directly proportional to the electric current induced in the circuit. In addition, the converter voltage V_{C_2} , the electrical charge stored in the converter capacitor can be calculated in terms of Q_{C_2} and C_2 capacitance as follows:

$$V_{C_2} = \frac{Q_{C_2}}{C_2} \quad (9)$$

D. Matlab/Simulink Model Implementation

The mathematical model of the proposed MEMS power inverter in Section C is implemented and solved using Matlab/Simulink software. The developed Simulink model consists of four separate parts. The first of these is the MEMS resonator, which represents the mass-damper-spring model used in normal MEMS systems. The mechanical actuation of the MEMS resonator only changes owing to the change in the electrostatic force of the system. The velocity and displacement values are examined according to the acceleration of the resonator. Here, the limit deviation function determines whether the resonator has undergone displacement or not. The second part is the variable capacitor part, where the circuit is completed by calculating the feedback of the circuit and the electrostatic force, which is the input terminal. The third part is the inverter circuit used to calculate the driver and converter capacitors of each circuit element according to the capacitance.

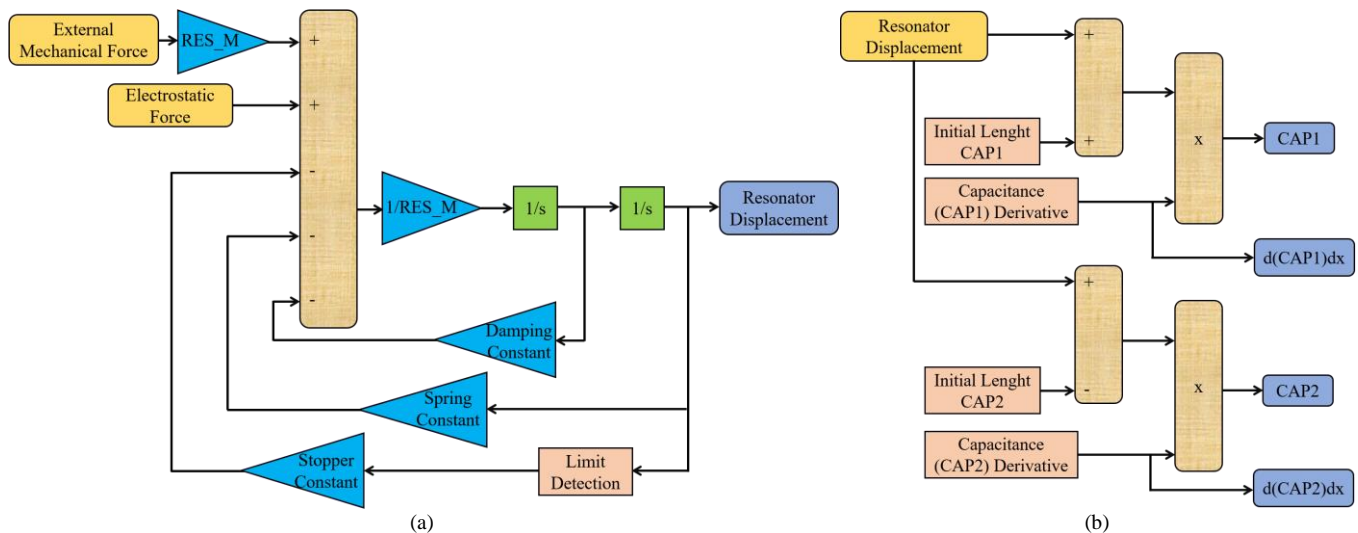


Fig.5. Simulink model of the mechanical resonator and variable capacitor (a) Mechanical resonator (b) Variable capacitor

The fourth part is the electrostatic force that occurs in the system when the MEMS resonator starts to work. The displacement of the MEMS resonator is used to extract the instantaneous values of the driver and converter capacitors at the input terminal.

The model of the MEMS resonator and the variable capacitor created in Simulink is given in Fig. 5. equations (1), (2), and (3) in Section mathematical modelling of MEMS power inverter calculate the velocity and displacement of the mass-spring-damper resonator according to its acceleration. The output of the block is zero when it does not reach the bias limit. When it reaches the deflection limit, it equals the collision force. There are two inputs in the block diagram, mechanical excitation, and electrostatic force. The mechanical excitation input expresses the vibration from the environment and is entered as zero in this simulation study. The other input is the electrostatic force obtained from the electromechanical model of the MEMS system. Another unit in Fig. 5 is the MEMS capacitor. In equations (5) and (6), the values of the converted capacitors that occur with the effect of the displacement of the MEMS capacitor are obtained. The input terminal of this unit is the displacement of the MEMS resonator. In addition, capacitance

derivatives are calculated according to the deviation required to calculate the electrostatic force of the system in equation (7).

The Simulink model of electric DC/AC inverter circuit and electrostatic force is given in Fig. 6. The electrical charge stored in the capacitor is calculated such that the voltage converted by equations (8) and (9) is proportional to the induced current. Thus, the voltage and current of each element in the circuit, driver capacitor, converter capacitor, and load resistance, are calculated. In this unit, AC reference voltage, solar cell voltage, driver, and converter capacitor values are applied as inputs. The other unit in Fig. 6 is the section where the electrostatic force is created. The power inverter system uses equation (7) to calculate the force. This force can be obtained.

The flow diagram of the MEMS power inverter modeled in Simulink in Section D is given below (Fig. 7). This diagram consists of the electrical actuation signal, electrostatic force, variable capacitor, MEMS resonator, power inverter circuit, solar cell system, and solar energy. In the initial position, the mechanical resonator is in equilibrium. This indicates that there is no displacement. A reference AC voltage is first applied to the power inverter system. The AC voltage is transferred to the section where the electrostatic force occurs.

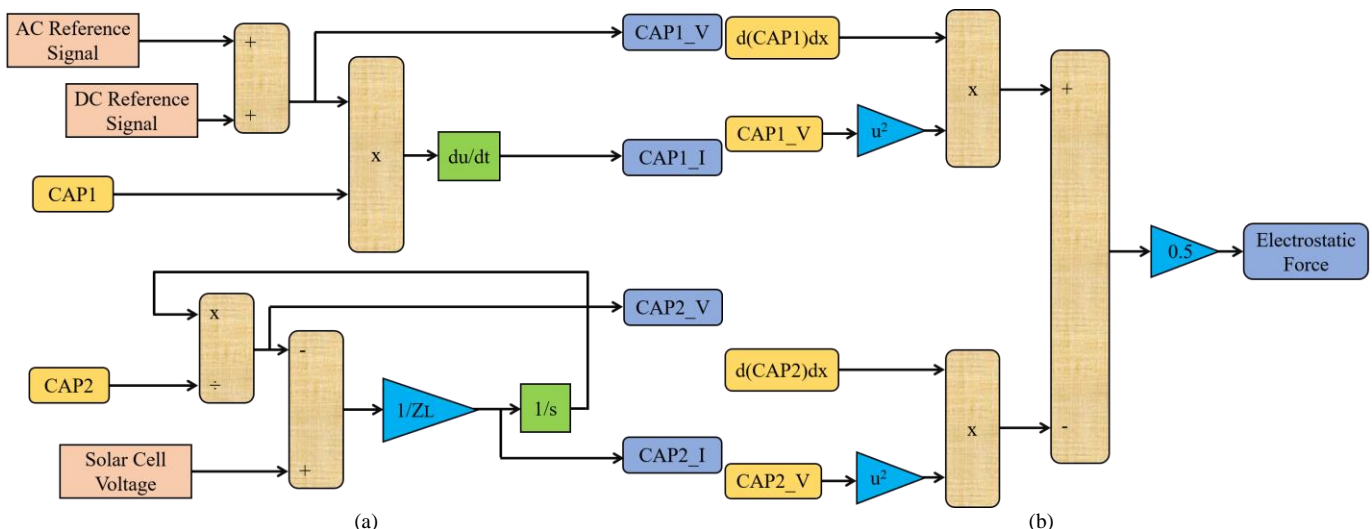


Fig.6. Simulink model of power inverter circuit and electrostatic force (a) Power inverter circuit (b) Electrostatic force

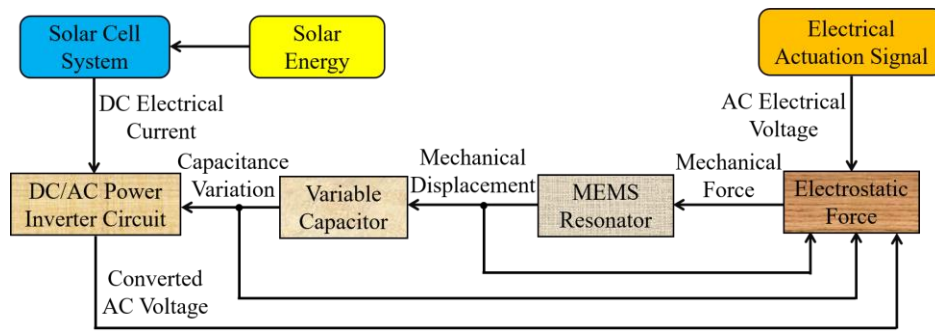


Fig.7. Signal flow schema of the Matlab/Simulink model

This section describes the unit that receives the mechanical feedback components from the MEMS resonator and the MEMS capacitor, the electrical feedback components from the electrical start signal, and the converted AC voltage from the electrical DC/AC inverter circuit. As the output of this unit, a mechanical vibration force is transferred to the MEMS resonator.

The output of the resonator block is the mechanical displacement signal transferred to the variable capacitor section for the calculation of new capacitor values. The result obtained by calculating the new values in the capacitor section is transferred to the DC/AC inverter circuit with the instantaneous capacitance value of the DC current coming from the solar cell system. As a result, the output voltage that emerges in the circuit with these inputs, i.e., the converted AC Signal, is calculated. This signal is transferred to the electrostatic force unit. Thus, the MEMS power inverter system is repeated without the need for a new AC reference voltage, and the DC/AC inverter is also converted.

III. RESULTS AND DISCUSSION

A. Simulation Results

In this section, the design and simulation results of a DC/AC inverter that can be used in renewable energy applications are presented. The design is analyzed in photovoltaic systems. As a result of the analysis, MEMS DC/AC inverter results close to the normal inverter were obtained. The graphical results of the mathematical model created to observe the effect of capacitance values were observed in Matlab/Simulink software by applying

different scenarios. The design criteria in Table 1 were used in all scenarios. As a result of the analysis, the change of capacitance according to displacement and electrical potential was examined. In addition, the efficiency of the voltage converted by the reference input voltage and the electrostatic force with the output signal was calculated.

Because the main frequency is 50 Hz in our country, the resonant frequency and the frequency of the reference AC voltage connected to the circuit are taken as 50 Hz. The MEMS residential area was chosen to be within the conventional dimensions. For the circuit to work, the main voltage connected to the circuit is 120 V AC, and the driver capacitance connected in series to the mains is 0.092 pF. The DC voltage from the solar panel can be between 0.5V and 48V. This study, the voltage converted according to the capacitance change at 0.5V and 24V DC voltages is simulated.

A comparison of the generated models was made using parameters such as electric potential distribution, displacement, and capacitance change. The potential electric distribution and displacement data are calculated for both models below with an operating voltage of 24 V. Two different models were designed for the capacitance analysis according to displacement. The results obtained from the compared models are shown in Fig. 8. The displacement increased as the capacitance value increased. The displacement and capacitance values are higher in Model 2. The 1st model showed an increase based on the max displacement range (1250 nm - 1260.62 nm), while the 2nd model showed an increase based on the max displacement range (2190 nm - 2193.885 nm).

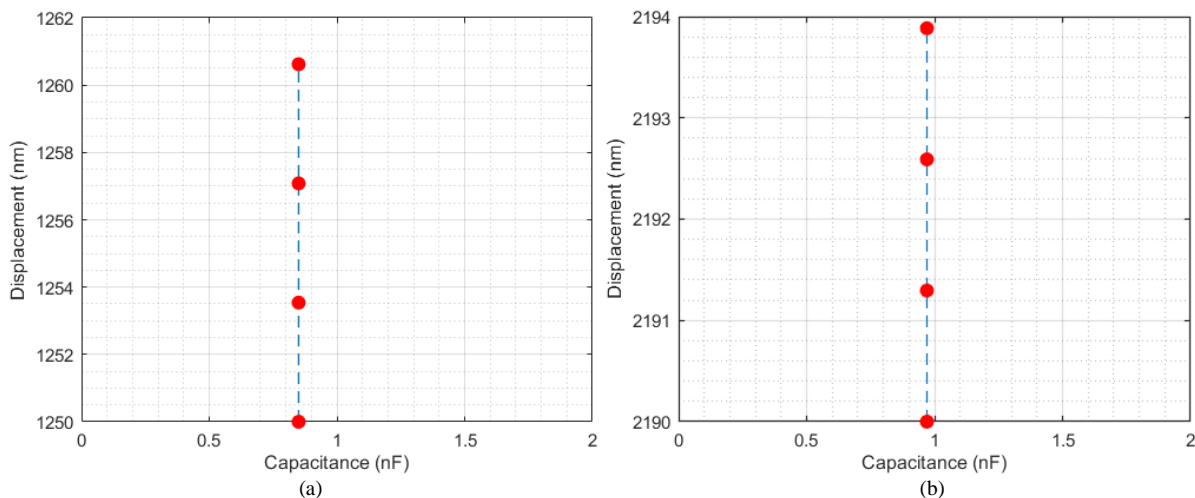


Fig.8. Capacitance values versus displacement for models (V=24V, C1=0.85nF, C2=0.97nF) (a) Displacements for model 1 (b) Displacements for model 2

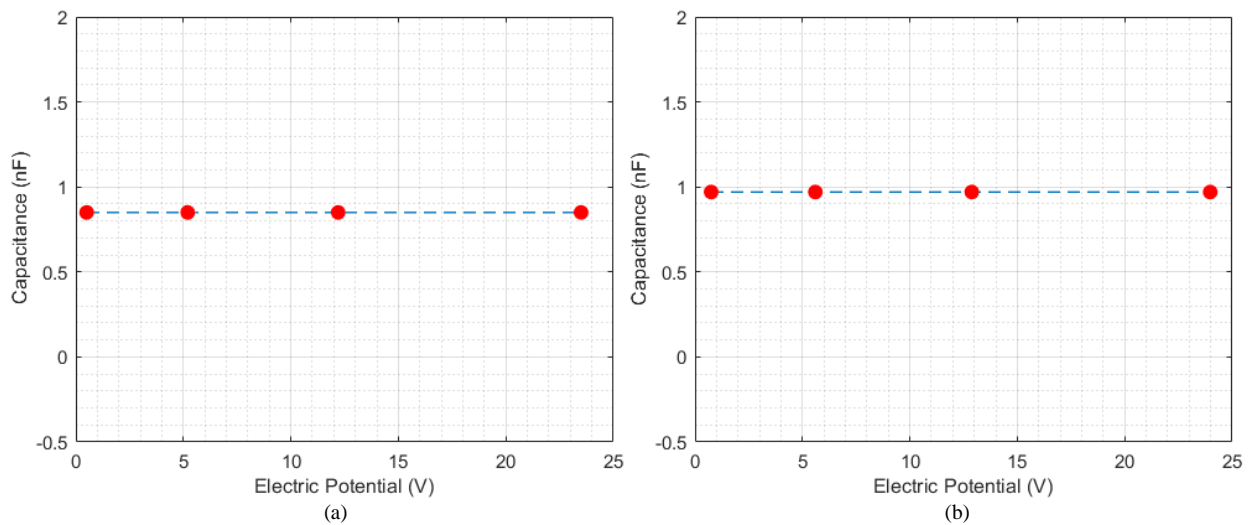


Fig.9. Electrical potential values versus capacitance for models (V=24V, C1=0.85nF, C2=0.97nF) (a) Capacitance for model 1 (b) Capacitance for model 2

Depending on the number of fingers in the MEMS comb structure, it shifted toward the Y axis with the increase in the overlap length of the capacitors overlapping in displacement.

Two different models were designed for capacitance analysis according to the electrical potential. The displacement depending on the capacitance value was investigated by selecting the input voltage as 24 V. The fixed and mobile electrons in the MEMS comb structure caused displacement on the surface and an increase in the electrical potential due to the change in capacitance. Since the increase in the electrical potential means the increase in the overlap area of the capacitors, the converter facilitates the increase of the capacitance throughout the circuit. The results obtained from the compared models are given in Fig. 9. As can be seen from the graphs, the electrical potential increases as the capacitance value increases. In addition, the electrostatic force and displacement increased as the capacitance increased according to the voltage changes between the electrical potential surfaces.

The electrostatic force and capacitance values of the moving electrodes were observed to change the capacitance caused by the fixed and moving electrodes. Since the reference AC voltage will cause vibration in the system, it will affect the electrostatic force. As the vibration coming to the resonator

increases, the electrostatic force will increase. Because of the operating voltage, the electrostatic force between the two electrodes is proportional to the square of the applied voltage. Its variation with different voltage values is given in Fig. 10a. The electrostatic force also causes displacement in the overlap length. This then causes a change in capacitance. Because the capacitance is inversely proportional to the voltage, its variation with voltage is shown in Fig. 10b. Developing low-power large-scale integration (VLSI) applications is critical to current technology [39]. The proposed MEMS power inverter model can be used for low-cost and low-power applications.

When the converted voltage analysis is performed according to the reference input voltage, a sinusoidal graph appears like a standard DC/AC inverter. In the simulation, a frequency of 50 Hz was applied. Initially, the input voltage was taken as 0V, and the output voltage conversion was provided at low capacitance values. The voltage-time graph converted at a capacitance value of 97 fF at a voltage of 0.5V DC is shown in Fig. 11a. Then, the capacitance value was increased by applying a voltage to the input. Again, a sinusoidal graph is obtained at the output. The voltage conversion graph of 0.5V DC voltage at 3900 fF with an input voltage of 120V is given in Fig. 11b.

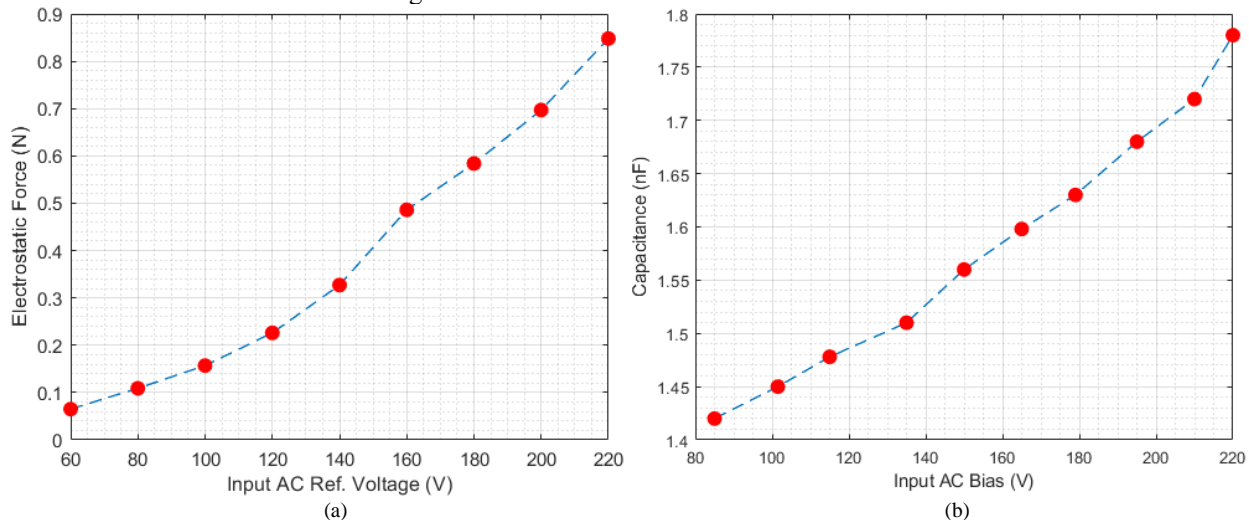


Fig.10. Electrostatic force and capacitance values versus reference voltage value (a) Electrostatic Force for model 1 (b) Capacitance for model 2

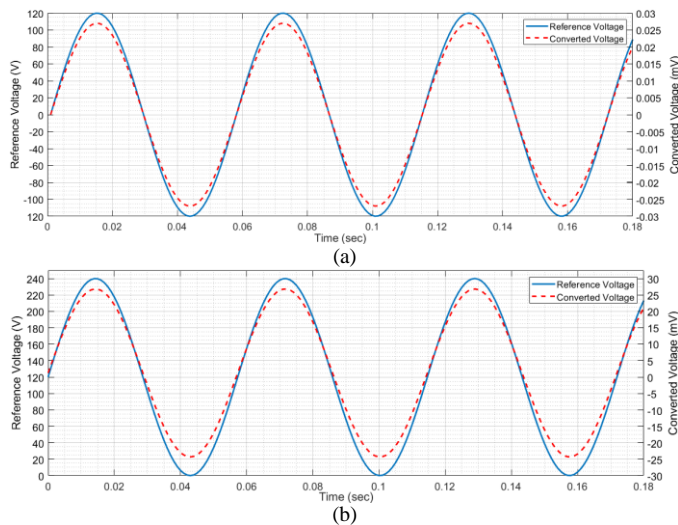


Fig.11. Voltage–time response simulation of MEMS inverter (a) Converted voltage graph versus 0 V reference input voltage (b) Converted voltage graph versus 120 V reference input voltage.

Finally, the efficiency performance of the MEMS power inverter is evaluated. Efficiency was calculated by changing the reference voltage and converting the capacitance values of the two different designs at 0.5 V DC voltage (Table II). The purpose of the designed inverter is to obtain the maximum AC amplitude signal from the DC input signal.

TABLE II
THE EFFICIENCY OF MEMS POWER INVERTER RELATIVE TO THE REFERENCE VOLTAGE

Efficiency (%)	V_L (mV)	V_{Dc} (V)	Converter capacitance (fF)	Reference voltage (V)
0.002828	0.02	0.5	97	0
0.002121	0.015	0.5	97	0
0.001414	0.01	0.5	97	0
0.000707	0.005	0.5	97	0
6.161728	43.57	0.5	3900	120
5.436237	38.44	0.5	3900	120
2.938736	20.78	0.5	3900	120
1.467954	10.38	0.5	3900	120

The efficiency of the design with the input voltage applied and the capacitance increased is better. Here, the efficiency (η), is calculated by the root mean square value of the DC input signal from the solar system and the resulting converted voltage V_L . The efficiency results calculated for capacitance changes at 0.5V voltage are given in Table 3. When the results were examined, it was determined that high efficiency could be obtained at high capacitance values. Tables II and III reveal that augmenting the converter capacitance enhances the efficiency of the MEMS power inverter, while elevating the supplied DC voltage notably amplifies the converted DC/AC voltage V_L .

TABLE III
THE EFFICIENCY OF THE MEMS POWER INVERTER RELATIVE TO THE DIFFERENT CAPACITANCE

Efficiency (%)	V_L (mV)	V_{Dc} (V)	Converter capacitance (fF)
0.0033	0.024	0.5	97
0.16	1.112	0.5	97
6.29	44.48	0.5	3900
6.3	44.54	0.5	3900

B. Discussion

A unique aspect of this work is the use of a capacitive MEMS-based power inverter designed for renewable energy applications. The use of MEMS technology in the field of power electronics is quite new, and little research has been done in this field. The role of power inverters in renewable energy systems is of great importance, and smaller, lighter and more efficient alternatives need to be investigated instead of traditional inverters. This study explores the potential of MEMS technology in power inverters and offers an original design for renewable energy applications. In addition, characterization of the inverter through simulation enables rapid evaluation of the performance of the design and provides valuable preliminary information before experimental prototype production. In this way, the efficiency of the design process increases and a more improved product is obtained.

In a study on how to improve the capacitive performance of MEMS-based transducers, MEMS-based DC/AC capacitive transducers of different materials and structures were tested [40]. At low input voltage, the capacitance increased due to curvature in the MEMS comb structure, which caused the deviation. In addition, the increase in the number of combs caused an increase in the electrostatic force. In the data obtained as a result of the simulation, the electrostatic force increased due to the increase in the number of combs and caused an increase in the capacitance. These results support the study. In another study, a MEMS-based low-power capacitive inverter design for renewable energy applications is presented, and the electrical and mechanical performances of two different MEMS structures are investigated by ignoring power losses at zero harmonic values [41]. In the study, less instability was obtained at the maximum displacement of the overlap length. In this article, the increase in the electrostatic force with the increase of the comb length was understood, and the efficiency and output signal obtained from the DC/AC inverter with the capacitance effect was examined. The results obtained are similar to this study. In a study on the efficiency calculation of MEMS power inverters, up to 6% efficiency was obtained [42]. In this study, efficiency was calculated in capacitance changes at 0.5V and 24V DC voltage, and it was determined that high efficiency could be obtained at high capacitance values. In this article, when the efficiency of the system was made by increasing the input voltage at 0.5V DC voltage and changing the capacitance values, it was observed that the efficiency increased as the capacitance value increased, and results similar to the study were obtained.

The simulation results and previous studies were compared, and it was understood how important capacitance is in MEMS technology. Depending on the capacitance, electrostatic force formation has been observed in MEMS devices. In renewable energy systems, the converted voltage in DC/AC inverters can benefit from MEMS technology to achieve maximum conversion with minimum loss. Elements affecting the designed DC/AC inverter have been determined, and it has been tried to use them in the most efficient way. With the mathematical equations and simulation results, the importance of the number and length of combs to be used in the MEMS system has been understood. The quality of the converted signal increases with the change in capacitance and electrostatic force.

As a result of simulation studies, the DC/AC conversion is possible with low-power applications.

This study discussed the design of a capacitive MEMS-based power inverter for renewable energy applications and its characterization through simulation. In the future, as an important continuation of this study, the design may need to be validated experimentally and the prototype tested in real environments. Field tests can be conducted to determine the performance of the inverter under real-world conditions and evaluate the effectiveness, reliability and integration ability of the optimized design. Additionally, a comprehensive study can be conducted examining the compatibility of the inverter with different renewable energy sources and its behavior under various operating conditions. However, innovative approaches such as improved control strategies or the use of new materials and manufacturing techniques can also be explored to increase the efficiency of the inverter. These studies can contribute to making renewable energy systems more efficient and reliable and promote progress in the field of MEMS-based power electronics.

IV. CONCLUSION

In this study, a capacitive MEMS-based power inverter design for renewable energy applications was developed, and characterization was carried out through simulation. Unlike conventional inverters, this inverter offers low costs, high efficiency, and low power consumption. The proposed inverter has a thickness of 325 μm , an active settlement area of 45x45x0.585 mm^3 , and an initial capacitance value of 2.9 pF. An electromechanical model was used to observe the voltage-time response of the power inverter. Simulation studies of the mathematical model created on this model were performed in Matlab/Simulink. In the simulation studies, the displacement, electrostatic force, and capacitance responses of the proposed MEMS inverter over different models were obtained. As a result of these findings, the power inverter transformed the DC voltage from the solar system into a true sinusoidal waveform and a perfect AC voltage signal with the AC signal of the power grid. Because the proposed inverter is based on a capacitive structure, it provides close to zero power consumption. As a result of the efficiency calculations, the frequency and waveform shape of the converted DC/AC signal was matched to the AC signal of a power grid with a conversion efficiency of 5%. The losses of the designed MEMS DC/AC inverter can be minimized by the material used, the number of combs, and their length. In addition, the efficiency can be further increased by changing the electrostatic force and choosing the appropriate input voltage and suitable capacitor. With MEMS technology, DC/AC inverters with a near-perfect sinusoidal wave output will be made for ease of maintenance, and inexpensive electronic devices will be produced by obtaining inverters with longer service life.

ACKNOWLEDGMENT

This study was conducted in the Siirt University Engineering Faculty Signal Processing Laboratory. I would like to take this opportunity to thank the Signal Processing Laboratory staff for their support.

REFERENCES

- [1] H. Husin, M. Zaki, "A critical review of the integration of renewable energy sources with various Technologies" Protection and Control of Modern Power Systems, vol. 6, 1, 2021, pp. 1-18.
- [2] B. K. Santhoshi, K. Mohanasundaram, L. A. Kumar, "ANN-based dynamic control and energy management of inverter and battery in a grid-tied hybrid renewable power system fed through switched Z-source converter" Electrical Engineering, vol. 103, 5, 2021, pp. 2285-2301.
- [3] M. H. Ahmed, M. Wang, M. A. S. Hassan, I. Ullah, "Power loss model and efficiency analysis of three-phase inverter based on SiC MOSFETs for PV applications" IEEE Access, vol. 7, 2019, pp. 75768-75781.
- [4] P. C. Vratny, H. Kuhn, M. Hornung, "Influences of voltage variations on electric power architectures for hybrid electric aircraft" CEAS Aeronautical Journal, vol. 8, 1, 2017, pp. 31-43.
- [5] K. J. Chen, O. Häberlen, A. Lidow, "GaN-on-Si power technology: Devices and applications" IEEE Transactions on Electron Devices, vol. 64, 3, 2017, pp. 779-795.
- [6] O. M. Rodriguez-Benítez, M. Ponce-Silva, J. A. Aquí-Tapia, A. Claudio-Sánchez, "Comparative performance and assessment study of a current-fed dc-dc resonant converter combining si, sic, and gan-based power semiconductor devices" Electronics, vol. 9, 11, 2020, pp. 1-15.
- [7] T. Kaliannan, J. R. Albert, D. M. Begam, P. Madhumathi, "Power quality improvement in modular multilevel inverter using for different multicarrier PWM" European Journal of Electrical Engineering and Computer Science, vol. 5, 2, 2021, pp. 19-27.
- [8] M. K. Das, K. C. Jana, A. Sinha "Performance evaluation of an asymmetrical reduced switched multi-level inverter for a grid-connected PV system" IET Renewable Power Generation, vol. 12, 2, 2018, pp. 252-263.
- [9] M. Pichan, H. Rastegar, "Sliding-mode control of four-leg inverter with fixed switching frequency for uninterruptible power supply applications" IEEE Transactions on Industrial Electronics, vol. 64, 8, 2017, pp. 6805-6814.
- [10] A. Sinha, K. C. Jana, M. K. Das, "An inclusive review on different multi-level inverter topologies, their modulation and control strategies for a grid connected photo-voltaic system" Solar Energy, vol. 170, 2018, pp. 633-657.
- [11] P. Shah, X. Zhao, "Leakage current mitigation technique in solar PV array system using passive filter" IEEE Transactions on Energy Conversion, vol. 38, 1, 2022, pp. 463-478.
- [12] M. U. Sardar, T. Vaimann, L. Kütt, A. Kallaste, B. Asad, S. Akbar, K. Kudelina, "Inverter-Fed Motor Drive System: A Systematic Analysis of Condition Monitoring and Practical Diagnostic Techniques" Energies, vol. 16, 15, 2023, pp. 5628.
- [13] F. Obeidat, "A comprehensive review of future photovoltaic systems" Solar Energy, vol. 163, 2018, pp. 545-551.
- [14] M. Dreidy, H. Mokhlis, S. Mekhilef, "Inertia response and frequency control techniques for renewable energy sources: A review" Renewable and Sustainable Energy Reviews, vol. 69, 2017, pp. 144-155.
- [15] Y. Slimani, A. Selmi, E. Hannachi, M. A. Almessiere, "Impact of ZnO addition on structural, morphological, optical, dielectric and electrical performances of BaTiO3 ceramics" Journal of Materials Science: Materials in Electronics, vol. 30, 10, 2019, pp. 9520-9530.
- [16] J. Druant, T. Vyncke, F. De Belie, P. Sergeant, J. Melkebeek, "Adding inverter fault detection to model-based predictive control for flying-capacitor inverters" IEEE Transactions on Industrial Electronics, vol. 62, 4, 2014, pp. 2054-2063.
- [17] Y. Liu, B. Ge, H. Abu-Rub, D. Sun, "Comprehensive modeling of single-phase quasi-Z-source photovoltaic inverter to investigate low-frequency voltage and current ripple" IEEE Transactions on Industrial Electronics, vol. 62, 7, 2014, pp. 4194-4202.
- [18] A. S. Abbas, R. A. El-Sehiemy, A. Abou El-Ela, E. S. Ali, "Optimal harmonic mitigation in distribution systems with inverter based distributed generation" Applied Sciences, vol. 11, 2, 2021, pp. 765-774.
- [19] Y. Peng, Y. J. Zhang, D. T. Liu, L. S. Liu, "Degradation estimation using feature increment stepwise linear regression for PWM Inverter of Electro-Mechanical Actuator" Microelectronics Reliability, vol. 88, 2018, pp. 514-518.
- [20] M. Chen, D. Zhou, F. Blaabjerg, "High penetration of inverter-based power sources with VSG control impact on electromechanical oscillation of power system" International Journal of Electrical Power & Energy Systems, vol. 142, 2022, 108370.

- [21] X. Guo, Q. Xun, Z. Li, S. Du, "Silicon carbide converters and MEMS devices for high-temperature power electronics: A critical review" *Micromachines*, vol. 10, 6, 2019, pp. 395-406.
- [22] I. V. Uvarov, A. N. Kupriyanov, "Stiction-protected MEMS switch with low actuation voltage" *Microsystem Technologies*, vol. 25, 8, 2019, pp. 3243-3251.
- [23] N. Gupta, S. Dutta, A. Panchal, I. Yadav, S. Kumar, Y. Parmar, "Design and fabrication of SOI technology based MEMS differential capacitive accelerometer structure" *Journal of Materials Science: Materials in Electronics*, vol. 30, 16, 2019, pp. 15705-15714.
- [24] W. Tian, P. Li, L. Yuan, "Research and analysis of MEMS switches in different frequency bands" *Micromachines*, vol. 9, 4, 2018, pp. 8-15.
- [25] I. E. Lysenko, A. V. Tkachenko, E. V. Sherova, A. V. Nikitin, "Analytical approach in the development of RF MEMS switches" *Electronics*, vol. 7, 12, 2018, pp. 395-415.
- [26] O. Ulkir, I. Ertugrul, N. Akkus, S. Ozer, "Fabrication and experimental study of micro-gripper with electrothermal actuation by stereolithography method. *Journal of Materials Engineering and Performance*, vol. 31, 10, 2022, pp. 8148-8159.
- [27] J. Yunas, B. Mulyanti, I. Hamidah, M. Mohd Said, R. E. Pawianto, "Polymer-based MEMS electromagnetic actuator for biomedical application: a review" *Polymers*, vol. 12, 5, 2020, pp. 1-18.
- [28] A. S. Algamili, M. H. M. Khir, J. O. Dennis, A. Y. Ahmed, S. S. Alabsi, "A review of actuation and sensing mechanisms in MEMS-based sensor devices" *Nanoscale Research Letters*, vol. 16, 1, 2021, pp. 1-21.
- [29] R. Sangno, R. K. Mehta, S. Maity, "MEMS Based Low Power Efficient Capacitive Inverter for renewable energy applications" *IEEE VLSI Circuits and Systems Letter*, vol. 5, 2, 2019, pp. 1-9.
- [30] G. Niu, F. Wang, "A review of MEMS-based metal oxide semiconductors gas sensor in Mainland China" *Journal of Micromechanics and Microengineering*, vol. 32, 5, 2022, pp. 1-25.
- [31] I. Vairavasundaram, V. Varadarajan, P. J. Pavankumar, R. K. Kanagavel, L. Ravi, S. Vairavasundaram, S. "A review on small power rating PV inverter topologies and smart PV inverters" *Electronics*, vol. 10, 11, 2021, pp. 1296.
- [32] U. Akram, M. Nadarajah, R. Shah, F. Milano, "A review on rapid responsive energy storage technologies for frequency regulation in modern power systems" *Renewable and Sustainable Energy Reviews*, vol. 120, 2020, pp. 109626.
- [33] H. Madinei, H. H. Khodaparast, M. I. Friswell, S. Adhikari, "Minimising the effects of manufacturing uncertainties in MEMS energy harvesters" *Energy*, 149, 2018, pp. 990-999.
- [34] E. Ranjbar, A. A. Suratgar, "A composite adaptive controller design for 3-DOF MEMS vibratory gyroscopes capable of measuring angular velocity" *Iranian Journal of Science and Technology, Transactions of Electrical Engineering*, vol. 43, 2, 2019, pp. 245-266.
- [35] A. Mustafazade, M. Pandit, C. Zhao, G. Sobreviela, "A vibrating beam MEMS accelerometer for gravity and seismic measurements" *Scientific Reports*, vol. 10, 1, 2020, pp. 1-8.
- [36] K. Tao, J. Miao, S. W. Lye, X. Hu, "Sandwich-structured two-dimensional MEMS electret power generator for low-level ambient vibrational energy harvesting" *Sensors and Actuators A: Physical*, vol. 228, 2015, pp. 95-103.
- [37] Y. Wang, H. Chen, B. Gao, X. Xiao, R. Torquato, F. C. Trindade, "Harmonic resonance analysis in high-renewable-energy-penetrated power systems considering frequency coupling" *Energy Conversion and Economics*, vol. 3, 5, 2022, pp. 333-344.
- [38] M. A. Haj-ahmed, M. S. Illindala, "The influence of inverter-based DGs and their controllers on distribution network protection" *In 2013 IEEE Industry Applications Society Annual Meeting*, 2013, pp. 1-9.
- [39] S. Vidhyadharan, R. Yadav, S. Hariprasad, S. S. Dan, "An advanced adiabatic logic using Gate Overlap Tunnel FET (GOTFET) devices for ultra-low power VLSI sensor applications" *Analog Integrated Circuits and Signal Processing*, vol. 102, 1, 2020, pp. 111-123.
- [40] R. Sangno, R. K. Mehta, S. Maity, "Improvement in capacitive performances of efficient micro electro mechanical system (MEMS) based power inverter" *Cogent Engineering*, vol. 5, 1, 2018, 1455407.
- [41] R. Sangno, R. K. Mehta, S. Maity, "MEMS Based Low Power Efficient Capacitive Inverter for renewable energy applications" *IEEE VLSI Circuits and Systems Letter*, vol. 5, 2, 2019, pp. 1-9.
- [42] H. A. Kloub, E. M. Hamad, "Electromechanical modeling and designing of capacitive MEMS DC/AC interactive power inverter for renewable energy applications" *Microsystem Technologies*, vol. 23, 4, 2017, pp. 863-874.

BIOGRAPHIES



Salih Rahmi Turan graduated from Kocaeli University, Engineering Faculty, Koala, in 2012 and received Ph.D. degree in Science and Engineering Institute from Marmara University, Istanbul, Turkey, in 2019. Now he works at Mus Alparslan University. His current research interests include micro electro mechanical system, additive manufacturing, renewable energy, additive manufacturing.



Osman Ulkir graduated from Kocaeli University, Engineering Faculty, Kocaeli, in 2012, and received M.Sc. degree from Marmara University, Institute of Pure and Applied Sciences, in Istanbul, Turkey, in 2015. He has been started Ph.D. studying in department of Mechatronics Engineering, Marmara University, Institute of Pure and Applied Sciences in 2015. He is currently working as an assistant professor in mechatronics engineering department at Mus Alparslan University. His special field of interest mechatronics system design, MEMS, biomechanics systems, signal processing, lower limb orthosis, additive manufacturing and data-driven predictive control.



Melih Kuncan received a B.S. degree in mechatronics engineering from Kocaeli University, Kocaeli, Turkey, in 2010, an MS degree in mechatronics engineering from Kocaeli University, Kocaeli, in 2013, and a Ph.D. degree in mechatronics engineering from Kocaeli University, Kocaeli, Turkey, in 2017. He is an Associate Professor in the Department of Electrical and Electronics Engineering, Siirt University. His areas of research include measurement, signal processing, medical signals, diagnosis, bearing fault, bearing fault diagnosis, fault classification and artificial intelligence.